

Ground-to-UAV Integrated Network: Low Latency Communication over Interference Channel

Sudhanshu Arya, *Member, IEEE* and Ying Wang *Member, IEEE*

Abstract—We present a novel and first-of-its-kind information-theoretic framework for the key design consideration and implementation of a ground-to-UAV (G2U) communication network with an aim to minimize end-to-end transmission delay in the presence of interference. The proposed framework is useful as it describes the minimum transmission latency for an uplink ground-to-UAV communication must satisfy while achieving a given level of reliability. To characterize the transmission delay, we utilize Fano’s inequality and derive the tight upper bound for the capacity for the G2U uplink channel in the presence of interference, noise, and potential jamming. Subsequently, given the reliability constraint, the error exponent is obtained for the given channel. In addition, as a function of the location information of the UAV, a tight lower bound on the transmit power is obtained subject to the reliability constraint and the maximum delay threshold. Furthermore, a relay UAV in the dual-hop relay mode, with amplify-and-forward (AF) protocol, is considered, for which we jointly obtain the optimal positions of the relay and the receiver UAVs in the presence of interference, and is compared with the point-to-point G2U link which ignores the relay. Interestingly, in our study, we find that, for both the point-to-point and relayed links, increasing the transmit power may not always be an optimal solution for delay minimization problems. In particular, we show that increasing the power gives a negligible gain in terms of delay minimization, though may greatly enhance the outage performance. Moreover, we prove that there exists an optimal height that minimizes the end-to-end transmission delay in the presence of interference. The proposed framework can be used in practice by a network controller as a system parameters selection criteria, where among a set of parameters, the parameters leading to the lowest transmission latency can be incorporated into the transmission. The based analysis further set the baseline assessment when applying Command and Control (C2) standards to mission-critical G2U and UAV-to-UAV (U2U) services.

Index Terms—Delay, latency, information-theoretic, interference, UAV.

I. INTRODUCTION

A. Background and Motivation

5G and beyond wireless systems are expected to support an ultra-reliable and low-latency communication link (URLLC) to enable uninterrupted and ubiquitous connectivity to mission-critical services where robust information exchange is important [1]. Indeed, the third generation partnership project (3GPP) aims to cover three generic connectivity technologies for 5G and beyond systems: URLLC, enhanced mobile broadband (eMBB), and massive machine-type communication (mMTC) [2]. eMBB is designed for

applications that have high requirements for the data rate, such as high-resolution video streaming whereas mMTC focuses on applications that support the massive number of machine-type devices with ultra-low power consumption. In contrast, URLLC is designed for delay-sensitive services and applications. For example, the services including intelligent transportation systems and tactile internet have reliability requirements of $(1 - 10^{-3}) \sim (1 - 10^{-9})$ at latency between 1 ms to 100 ms [3]. However, due to the dynamic and fast-fading channel, shadowing, and path loss over wireless links, it becomes challenging to meet the quality-of-service (QoS) requirement for URLLC systems.

To meet the challenging demands of 5G wireless networks, 3GPP has recommended integrating unmanned aerial vehicles (UAVs) into wireless cellular networks [4]. With a high probability of establishing a LOS communication link, UAVs are more likely to provide better link quality over short-distance. Moreover, UAVs are generally cost-effective and offer more flexibility for on-demand communication systems in low-altitude environments. As a result, UAVs have received significant research attention in wireless communications [5], [6].

A system model for UAV relay-assisted IoT networks was presented to primarily explored the impact of requested time-out constraints for uplink and downlink transmissions [7]. A problem to maximize the total number of served IoT devices was formulated. The authors jointly optimized the transmission power, trajectory, system bandwidth, and latency constraints for the full-duplex UAV-assisted IoT devices. In another work, a single-hop and multi-hop relay-assisted UAV network with a ground-based transmitter and receiver, the problem of finding the optimal UAV location to minimize the impact of interference was investigated [8]. A theoretical framework was presented to determine the minimum number of UAVs required and their optimal locations to meet the minimum requirement of the received average signal-to-interference ratio. Considering a heterogeneous wireless network of a ground base station, relay aerial vehicles, and a high-altitude platform, the end-to-end delay and reliability analysis of downlink communication links was investigated [9]. It was demonstrated that even with a very efficient interference mitigation technique employed, the current wireless networks designed for terrestrial users are not suitable to meet the URLLC requirements for downlink control communication to aerial vehicles.

To improve the communication performance and network connectivity for the ground nodes or vehicles in a 3D urban scenario, particle swarm optimization was utilized to find the optimal UAV positions functioning as relay nodes [10]. To

arXiv:2305.02451v1 [cs.IT] 3 May 2023

(Corresponding author: Ying Wang.)

Sudhanshu Arya and Ying Wang are with the School of Systems and Enterprises, Stevens Institute of Technology, Hoboken, USA (e-mail: sarya@stevens.edu; ywang6@stevens.edu).

validate the proposed approach, an indoor experiment was also conducted. However, it is to be noted that, there were no communications among the relayed UAVs. In another work, a model predictive control approach was utilized to construct an energy-efficient communication link between the ground nodes with UAV operating as a relay node [11]. In particular, a problem was formulated to optimize the source's transmit energy and the UAV's propulsion energy by jointly optimizing the UAV's mobility and transmission across the multiple access channel. However, the approach was limited to a linear trajectory where it was assumed that the UAV is moving along a single dimension at a fixed height with no lateral displacement. In [12], a throughput maximization problem was formulated for a UAV-assisted mobile relay network. The problem was based on jointly optimizing the trajectory of the relay UAV node and the power allocation of the source and relay node, subject to the information-causality constraints. In particular, the authors considered two scenarios. In the first scenario, the relay trajectory was kept fixed, and it was shown that the optimal source and UAV power allocations obey a staircase water-filling structure with non-increasing and non-decreasing power levels at the source and UAV, respectively. Whereas, in another scenario, an iterative algorithm was presented to jointly optimize the UAV trajectory and the power allocation in an alternating way. In another similar work [13], however, considering the circling operation of the fixed-wing UAV, a rate optimization approach is presented for UAV enabled wireless relay network. It was assumed that there is no direct link between the ground-based source and the destination. A variable rate protocol was developed to optimally adjust the data rate depending on the location of the UAV. It was shown that the proposed approach significantly outperforms the conventional fixed-rate relaying network.

Since there is no regulatory and well-defined pre-allocated spectrum band for UAV communications, it makes constructing a UAV-assisted communication network a non-trivial task. Therefore, UAV-assisted network generally coexists with other wireless networks, e.g., cellular networks [14]. Thus, formulating the problem of delay minimization given the reliability constraint is critical. This is the main fact that motivated us in formulating the information-theoretic-based framework to investigate the end-to-end transmission delay in the presence of interference. Utilizing our existing outdoor 5G testbed [?], Over the Air (OTA) verification and extension of the proposed work is being performed.

B. Contributions

Unlike traditional terrestrial or satellite communication networks, the air-to-ground integrated network is affected by the limitations arising simultaneously from the following segments, i.e., from the aspects of mobility management, power control, and end-to-end QoS requirements. Therefore, given the practical resource constraints of an air-to-ground integrated network, it is critically important for an integrated network to achieve optimal and reliable performance given the restriction in power consumption. Therefore, optimal system integration

and network design and configuration are of great significance in an air-to-ground and air-to-air integrated network. To this end, we present a novel information-theoretic approach to the design of an optimal air-to-ground integrated network that assesses and minimizes end-to-end transmission latency in the presence of interference, white noise, and potential jamming. The main contributions of this paper are listed below.

- We present an information-theoretic framework for the design of an optimal ground-to-UAV communication network that minimizes end-to-end transmission delay. The proposed framework is useful as it describes the minimum transmission latency a UAV network must satisfy while achieving a given level of reliability in terms of the average error probability. In particular, we first derive a tight upper bound for the capacity of the air-to-ground integrated channel in the presence of interference and white noise. Subsequently, given the reliability constraint, a framework is developed to analyze the delay introduced in the channel.
- Further, considering the general air-to-ground network with inter-relay communication, the results are presented to comprehensively characterize the optimal performance of the system towards end-to-end delay minimization. We show that despite the simplicity of the point-to-point direct link, the latency of the amplify-and-forward (AF) relayed-based link can be lower if the relay is properly located.
- In addition, we considered the power consumption restriction in the air-to-ground and air-to-air networks. Within the range of allowable system latency, the optimal transmit power is derived based on the location information of a UAV. From the analysis, it is shown that increasing the transmission power is not always the proper solution to the delay minimization problem.

The rest of the paper is organized as follows. In Section II, we present the system model. The delay analysis is presented in Section III whereas results and discussions are depicted in Section IV. Finally, the conclusion is drawn in Section V.

II. SYSTEM MODEL

We consider an interference network where a transmitted signal is corrupted by the interference signal plus the additive white Gaussian noise (AWGN). In this noise-plus interference-limited network, there can be two types of communication links: a direct link from the ground base station (BS) to the receiver UAV and a relay-assisted link from the BS to the receiver UAV. Let the ground BS, located at $(x_T, y_T, 0)$, communicates to the receiver (R_x) located at (x_R, y_R, z_R) in the presence of interfering nodes located at $(x_I^{(i)}, y_I^{(i)}, 0), i \in \Phi_I$. Φ_I is a subset containing all interfering nodes transmitting at time t .

Let the BS transmits with power P_T over a channel with path loss exponent α_T and fading coefficient h_T . $d_T = \sqrt{(x_T - x_R)^2 + (y_T - y_R)^2 + (z_T - z_R)^2}$ is the distance between the BS and R_x . s_T is a code word of length N and is a sequence of N numbers such that $s_T = (s_{T_1}, s_{T_2}, \dots, s_{T_N})$. The code word s_T for an underlying ground-to-UAV channel

TABLE I: Notations

Parameter	Description
d_c	Block length of the code word s_T
R_c	Code rate
P_T	Transmit power
$P_I^{(i)}$	Transmit power of the i th interfering node
P_N	Power of the amplifying node
ϕ_e	Reliability constraint
Φ_I	Number of active interfering nodes at any time t
$h_{u,v}$	channel gain between the nodes u and v
$\alpha_{u,v}$	Path loss exponent of the link $u \rightarrow v$
$\alpha_{I,v}^{(i)}$	Path loss exponent of the link between the i th interferer and the v th receiver
$\theta_{u,v}$	Elevation angle between the transmitting node u and the receiving node v
$\theta_{I,v}^{(i)}$	Elevation angle between the receiver v and the i th interfering node
$d_{u,v}$	3D distance between the nodes u and v
$w_R(t)$	AWGN noise at the input of the receiver
$w_N(t)$	AWGN noise at the input of the relay node
N_0	Noise spectral density
B_{uv}	Link bandwidth between the nodes u and v
$d_{u,v}$	3D distance between the nodes u and v
B	Information bits in a codeword message of length d_c

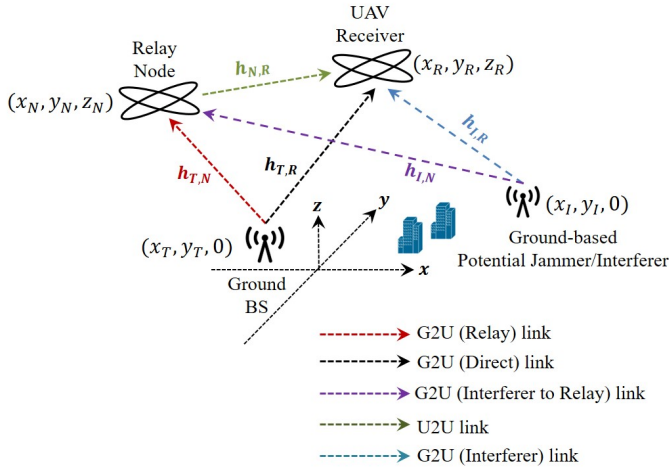


Fig. 1: Illustration of the system model.

may be thought of geometrically as a point in N -dimensional Euclidean space. The impact of the channel impairment due to the Gaussian noise and interference is then to move s_T to a nearby point according to a spherical Gaussian distribution. $s_T(t)$ are random symbols drawn from a constellation size M with unitary mean power. $P_I^{(i)}$ denotes the transmit power of the i th interfering node.

We consider an AF relay channel with one hop, as illustrated in Fig. 1. To avoid interference between the ground BS and the relay, it is assumed that the information transmission is conducted via time division where the transmission from the ground BS to the receiver is divided into two time slots. In

the first slot, the signal is received by the relaying UAV, which is then amplified, and in the second slot, the amplified signal is received by the receiver UAV. An arbitrary relay UAV can normalize and re-transmit the received signal. With the power P_N , the re-transmitted signal s_N is represented by

$$s_N(t) = \frac{\sqrt{P_N} Y_N(t)}{\sqrt{E[|Y_N(t)|^2]}} = \frac{\sqrt{P_N} \left(\sqrt{P_T d_{T,N}^{-\alpha_{T,N}(\theta_{T,N})}} h_{T,N} s_T(t) + w_N(t) \right)}{\sqrt{P_T d_{T,N}^{-\alpha_{T,N}(\theta_{T,N})} |h_{T,N}|^2 + B_{TN} N_0}} \quad (1)$$

where P_T is the transmit power of the ground BS and w_N denotes the white noise at the input of the relaying UAV. $E[\cdot]$ represents the expectation operation. Following (2), the signal received at the receiver is expressed as

$$Y_R(t) = s_N(t) \sqrt{d_{N,R}^{-\alpha_{N,R}(\theta_{N,R})}} h_{N,R} + \sum_{i \in \Phi_I} \sqrt{P_I^{(i)} d_{i,R}^{-\alpha_{I,v}^{(i)}(\theta_{I,v}^{(i)})}} h_{I,R}^{(i)} s_I^{(i)}(t) + w_R(t) \quad (2)$$

We consider that the G2A and the A2A communication links experience LOS propagation with LOS probability $P_{LOS,h}$, $h \in \{h_T, h_{T,N}, h_{N,R}, h_{I,R}, h_{I,N}\}$, expressed as [16]

$$P_{LOS,h} = \frac{1}{1 + f_1 \exp(-f_2(\theta_h - f_1))} \quad (3)$$

where f_1 and f_2 are environment-dependent parameters determined by the building density and heights. Due to the LOS path for all the described links, the small-scale channel fading gain h can be assumed to follow the Rician model with PDF given by

$$f_h(h) = \frac{h}{\sigma_h^2} \exp\left(-\frac{h^2 + \rho_h^2}{2\sigma_h^2}\right) I_0\left(\frac{h\rho_h}{\sigma_h^2}\right), h \geq 0, \quad (4)$$

where σ_h and ρ_h represent the strength of the LOS and NLOS components. $I_0(\cdot)$ is the zeroth order modified Bessel function of the first kind. Following (4), the Rice factor K_h (dB) of any link $h \in \{h_{T,R}, h_{T,N}, h_{N,R}, h_{I,R}, h_{I,N}\}$, can then be defined as K_h (dB) = $10 \log_{10}\left(\frac{\rho_h^2}{2\sigma_h^2}\right)$. We like to point out that the Rice factor K_h is a function of the parameters such as the carrier frequency and the elevation angle θ_h [9].

We define the instantaneous signal-to-noise ratio (SNR) of arbitrary link $u \rightarrow v$, from the transmitter u , $u \in \{T, N\}$ to the receiver v , $v \in \{N, R\}$, over the known interference channel as

$$\lambda_{uv} = \frac{\left| \sqrt{P_u d_{u,v}^{-\alpha_{u,v}(\theta_{u,v})}} h_{u,v} \right|^2}{B_{uv} N_0}, \quad (5)$$

and the power ratio between the intended received signal at v , $v \in \{N, R\}$ from u , $u \in \{T, N\}$, and the interference signal from the i th interfering node is expressed as

$$\gamma_{uv}^{(i)} = \frac{\left| \sqrt{P_u d_{u,v}^{-\alpha_{u,v}(\theta_{u,v})}} h_{u,v} \right|^2}{\left| \sum_{i \in \Phi_I} \sqrt{P_I^{(i)} d_{i,v}^{-\alpha_{I,v}^{(i)}(\theta_{I,v}^{(i)})}} h_{I,v}^{(i)} \right|^2}. \quad (6)$$

The expression in (6) is general enough to be treated as a signal-to-interference ratio (SIR).

Averaging over the fading statistics described in (4), we obtain the average received SNR $\bar{\lambda}_{uv}$ as illustrated in (7). $G_{m,n}^{s,t}[\cdot]$ in (7) represents the Meijer G-function [17]. The derivation steps are provided in Appendix A.

III. DELAY ANALYSIS

The critical and important questions we would like to answer in this work are: What is the transmission latency of the G2U communication link under the given system parameters? And what are the optimal locations of the relay and the UAV to have a positive impact in minimizing the transmission delay? More precisely, our objective is to minimize the delay in transmitting messages between the transmitter and the receiver in UAV communication while guaranteeing a required level of reliability ϕ_e , such that,

$$P_e(d_c, R_c) \leq \phi_e, \quad (8)$$

where $P_e(d_c, R_c)$ represents the average error probability of the code with length d_c and rate R_c . The channel code rate R is a function of the input target signal distribution f_T , the input interference signal distribution f_I , λ , and γ . The channel code rate R_c is achievable if there is an encoding function to map each transmitted message S to s_T and there is another decoding function to map each received signal Y and interference information to a transmitted message as \hat{S} , such that the average error probability $P_e(d_c, R_c) \triangleq P_r[S \neq \hat{S}] \rightarrow 0$ when N goes large. Following this, we define the reliability function in terms of the error exponent of the channel as [18]

$$E(R_c) = - \lim_{d_c \rightarrow \infty} \sup \frac{\ln P_{e,\min}(d_c, R_c)}{d_c}, \quad (9)$$

where $\sup(\cdot)$ represents the supremum function and $P_{e,\min}(d_c, R_c)$ denotes the infimum or the greatest lower bound of the error probability over all (d_c, R_c) codes for a given d_c and R_c . It can be readily shown that the error exponent depicted in (3) is upper bounded by the sphere packing exponent

$$E(R_c) \geq \max_{\rho > 0} \{E_0(\rho) - \rho R_c\}, \quad (10)$$

where

$$E_0(\rho) = - \log \int_{-\infty}^{\infty} \left(\int (P(Y_R | s_T))^{\frac{1}{1+\rho}} dP(s_T) \right)^{1+\rho} dY_R \quad (11)$$

where $P(s_T)$ denotes the cumulative distribution function of the input s_T and $P(Y_R | s_T)$ is the probability density (or mass) function of the output Y given the input s_T . ρ is a parameter, $0 \leq \rho \leq 1$, and should be selected such that d_c is minimized. Utilizing (7), (8), and (10), and applying the identity [19, eq. 11], the minimum transmission delay introduced into the channel in order to satisfy the reliability constraint is given by

$$d_c \geq \frac{\rho B - \log \phi_e}{G_{2,2}^{1,2} \left[\bar{\lambda}_{uv} \left| \begin{array}{l} 1, 1 \\ 1, 0 \end{array} \right. \right]}, \quad (12)$$

where B represents the information bits in the codeword of length d_c .

We define the capacity of the uplink ground-to-UAV channel impaired by the known interference as

$$C(\lambda, \gamma) = \sup_{f_T} \left[\inf_{f_I} R_c(f_T, f_I, \lambda, \gamma) \right] \quad (13)$$

subject to $\mathbb{E}[s_I]^2 = 1, \mathbb{E}[s_T]^2 = 1$

Next, we present a tight upper bound for $C(\lambda, \gamma)$ defined in (13).

To decode the transmitted message S correctly with a low probability of error, the conditional entropy $H(S|Y_R, s_I)$ has to be close to zero [20]. Following this, and applying Fano's inequality [21] into the definition of channel entropy, it can be readily shown that

$$d_c R_c(f_T, f_I, \lambda, \gamma) \leq I(S; Y_R, s_I) + d_c \zeta_{d_c}, \quad (14)$$

where ζ_N is the error detection parameter satisfying the condition $\lim_{d_c \rightarrow \infty} \zeta_{d_c} = 0$. Applying the definition of mutual information and utilizing the fact that S and s_I are independent, (14) can be written as

$$d_c R_c(f_T, f_I, \lambda, \gamma) \leq H(Y_R | s_I) - H(Y_R | S, s_I) + \zeta_{d_c}, \quad (15)$$

where $H(Y_R | s_I)$ can be interpreted as the uncertainty in Y conditional on s_I . $H(Y_R | S, s_I)$ accounts for the reduction in uncertainty of Y conditional on s_I from the observation of s_I . Substituting the expressions for $H(Y_R | s_I)$ and $H(Y | S, s_I)$ into (15), the tight upper bound for the capacity of the air-to-ground channel is derived as illustrated in (16). N_p in the summation term in (16) denotes the packet length. T_c represents the block of symbols over which the channel is assumed to be constant. The detailed derivation steps of (16) are provided in Appendix A.

We like to point out that, since the channel is random over a single transmission interval with the assumption that the channel state information is not available to the BS, and considering the capacity as defined in (13), it is now possible that $C(\lambda, \gamma) = 0$ with nonzero probability irrespective of the link range and transmission power. Therefore, the power allocation approach may not be an optimal solution for the uplink G2U networks. Moreover, it is now impossible to guarantee successful information transmission with $\phi_e = 0$ and $C(\lambda, \gamma) > 0$.

Next, we obtain the minimum transmit power $P_{u,\min}$ required at node u , given the maximum allowable delay $d_{c,\max}$ and the reliability constraint ϕ_e at the receiver v . Following (2), (10), and (11), the tight upper bound on the transmit power requirement, subject to the reliability constraint and the maximum delay threshold, can readily be derived as shown in (17).

IV. RESULTS AND ANALYSIS

The simulation parameters are summarized in Table II. We consider a slow-fading channel, where the actual channel gains are assumed to be constant, however, random over a single transmission interval. Unless otherwise stated, the interferer

$$\bar{\lambda}_{uv} = \frac{\sqrt{P_u d_{u,v}^{-\alpha_{u,v}(\theta_{u,v})}} (-2\pi\sigma_{h_{u,v}}^2)}{B_{uv}N_0} \exp\left(-\frac{\rho_{h_{u,v}}^2}{2\sigma_{h_{u,v}}^2}\right) G_{3,4}^{2,1} \left[\frac{2\rho_{h_{u,v}}^2}{\sigma_{h_{u,v}}^2} \mid \begin{matrix} -2, -1, \frac{1}{2} \\ 0, -2, 0, \frac{1}{2} \end{matrix} \right]. \quad (7)$$

$$R_{c,uv} \leq \frac{(T_c - 1)}{T_c} \log \left(1 + \frac{P_u d_{u,v}^{-\alpha_{u,v}(\theta_{u,v})} \|h_{u,v}\|^2}{B_{uv}N_0} \right) + \frac{1}{N_p} \sum_{j=1}^{N_p/T_c} E_{s_{I,j}} \left[\log \left(1 + \frac{P_u d_{u,v}^{-\alpha_{u,v}(\theta_{u,v})} \|h_{u,v}\|^2}{\sum_{i \in \Phi_I} P_I^{(i)} d_i^{-\alpha_{I,v}(\theta_{I,v}^{(i)})} \|h_{I,v}^{(i)}\|^2 \|s_{I,j}\|^2 + B_{uv}N_0} \right) \right] + \zeta_{d_c}. \quad (16)$$

$$P_{u,\min} \geq \left\{ (1 + \rho) \exp\left(\frac{\rho B - \log \phi_e}{d_{c,\max}}\right) \left(\left| \sum_{i \in \Phi_I} \sqrt{P_I^{(i)} d_{I,v}^{-\alpha_{I,v}(\theta_{I,v}^{(i)})}} h_{I,v}^{(i)} \right|^2 + B_{uv}N_0 \right) - 1 \right\} \frac{1}{d_{u,v}^{-\alpha_{u,v}(\theta_{u,v})} \|h_{u,v}\|^2}. \quad (17)$$

$$\bar{\lambda}_{u,v} = \frac{\sqrt{P_x d_{u,v}^{-\alpha_{u,v}(\theta_{u,v})}}}{B_{uv}N_0} \left(\frac{\pi}{\sigma_{h_{u,v}}^2} \right) \exp\left(-\frac{\rho_{h_{u,v}}^2}{2\sigma_{h_{u,v}}^2}\right) \left\{ \int_0^\infty \underbrace{\left[h_{u,v}^3 G_{1,3}^{1,0} \left[h_{u,v}^2 \frac{\rho_{h_{u,v}}^2}{\sigma_{h_{u,v}}^2} \mid \begin{matrix} \frac{1}{2} \\ 0, 0, \frac{1}{2} \end{matrix} \right] \right]}_{\text{Term I}} - \underbrace{\left[h_{u,v}^3 G_{1,2}^{1,1} \left[\frac{h_{u,v}^2}{2\sigma_{h_{u,v}}^2} \mid \begin{matrix} 1 \\ 1, 0 \end{matrix} \right] G_{1,3}^{1,0} \left[h_{xy}^2 \frac{\rho_{h_{u,v}}^2}{\sigma_{h_{u,v}}^2} \mid \begin{matrix} \frac{1}{2} \\ 0, 0, \frac{1}{2} \end{matrix} \right] \right]}_{\text{Term II}} \right\} dh_{u,v}. \quad (18)$$

TABLE II: System Parameters

Parameter	Value
Packet size	32 bytes
Rice factor of G2A link	5 ~ 12 dB
Rice factor of A2A link	10 ~ 12 dB
Noise spectral density N_0 [9]	-174 dBm/Hz
LOS (NLOS) shadow fading standard deviation	4 (6) dB
Model parameter f_1 [22]	12.08
Model parameter f_2 [22]	0.11
Carrier frequency f_c	2 GHz

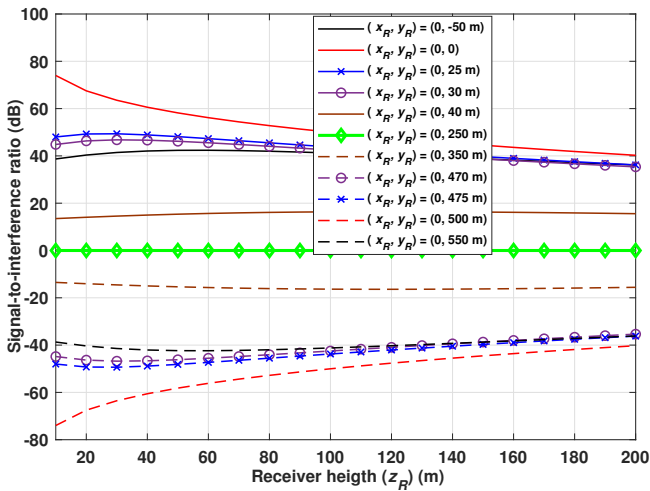


Fig. 2: Signal-to-interference ratio relative to the receiver height for different y_R along the line joining the transmitter and the interferer.

coordinates are set to $(0, 500, 0)$. To get a satisfactory statistical average, for each link configuration parameter set, 1000 realizations of normal distributed independent random variables are generated. The delay is then obtained by averaging the results over 1000 realizations. For brevity, we assume one interfering node. For simplicity, we consider the following three cases to describe the link geometries.

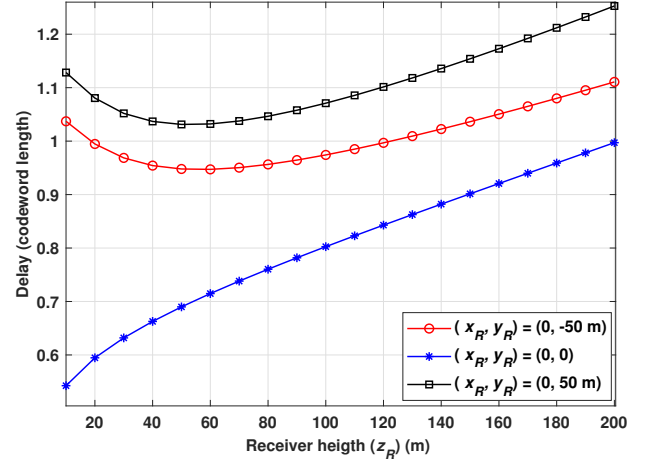
- **Case I:** It considers a scenario where the receiver is located above in a region near the vicinity of the transmitter
- **Case II:** It considers a scenario where the receiver is located above in a region near the midway of the line joining the transmitter and the receiver
- **Case III:** It considers a scenario where the receiver is located above in a region near the vicinity of the interfering node

Fig. 2 shows the SIR variation with receiver height (z_R) at different positions along the line joining the BS and the interferer. For Case I, as z_R increases, the signal of interest becomes weaker, and hence, the interference becomes relatively stronger. On the contrary, for Case III, increasing z_R results in a weaker interference thereby making the signal of interest relatively stronger and hence higher SIR. However, the nearly constant SIR for case II can be attributed to the fact that both, the signal of interest and the interference signal, become weak proportionally with increasing z_R .

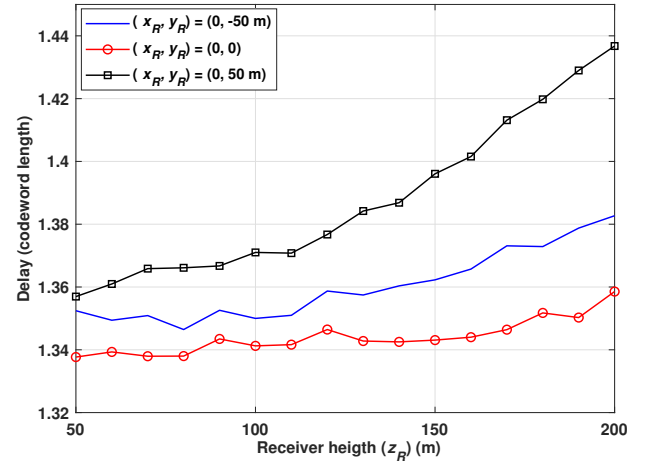
In Fig. 3a, 3b, and 3c, we show the results for the delay, while varying the receiver height z_R for several channel conditions, i.e., over the interference-limited channel, and when $\bar{\lambda} = 30$ dB and $\bar{\lambda} = 0$ dB, respectively. In Fig. 3a, as expected, we can observe that for an interference-limited channel, when the receiver is located above the transmitter, the delay is an increasing function of the receiver height. In contrast, when the receiver moves in either direction in a line joining the transmitter and the interferer, the delay shows non-monotonic behaviors with the receiver height. Indeed, for the given link configuration and the placements of the ground BS and the interferer, the delay first decreases with increasing the height till the optimal height is obtained and then increases with the height. This quasi-monotonic behavior can be attributed to the fact that increasing the receiver height beyond the optimal height causes higher interference and path loss. In contrast to the interference-limited channel, slightly different trends are observed in the interference-plus-noisy channel. For example, in Fig. 3b, when $\bar{\lambda} = 30$ dB, the delay increases with z_R irrespective of x_R and y_R , however, in Fig. 3c, when $\bar{\lambda}$ is very low, the three curves, however, cannot be distinguished. It shows that noise is a dominating factor in this case.

Figure 4 presents the end-to-end delay profile relative to the receiver height for the direct link over different channel conditions for Case II. The different curves in Fig. 4a and 4b demonstrate the impact of varying the receiver along the midpoint on the line joining the transmitter and the interferer. Based on the results, a few important observations can be made.

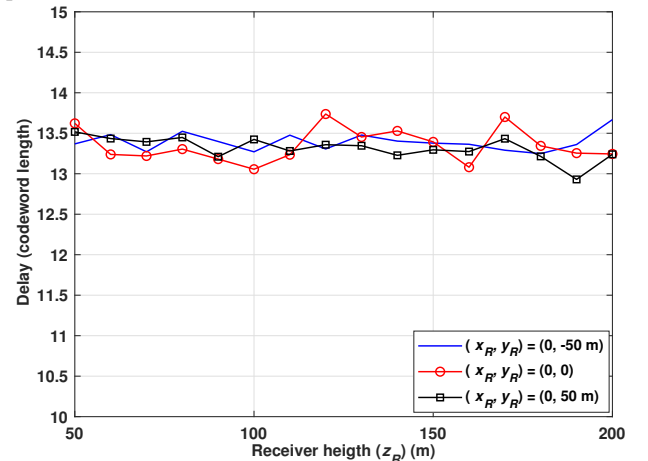
- If the UAV is located near the midpoint such that, $d_{T,N} > d_{i,R}$, the delay first increases rapidly with the height and then decreases gradually with further increasing the UAV height. This monotonic behavior can be attributed to the fact that increasing the height initially causes received signal power to decrease relatively at a higher rate than interference and thereby reduces the number of packets successfully received. However, at larger heights, the impact of the interference signal also reduces, thus causing the delay to decrease gradually.



(a) Interference-limited channel.

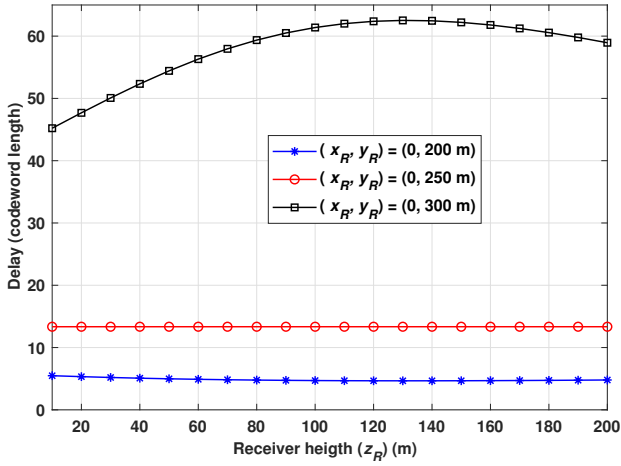


(b) Interference channel with end-to-end received signal-to-noise power ratio $\lambda = 30$ dB.



(c) Interference channel with end-to-end received signal-to-noise power ratio $\lambda = 0$ dB.

Fig. 3: Delay profile as a function of the receiver height over different channel conditions (Case I).



(a) Interference-limited channel.

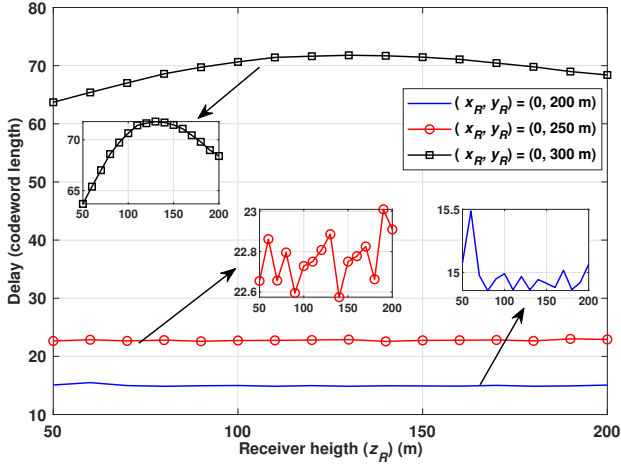
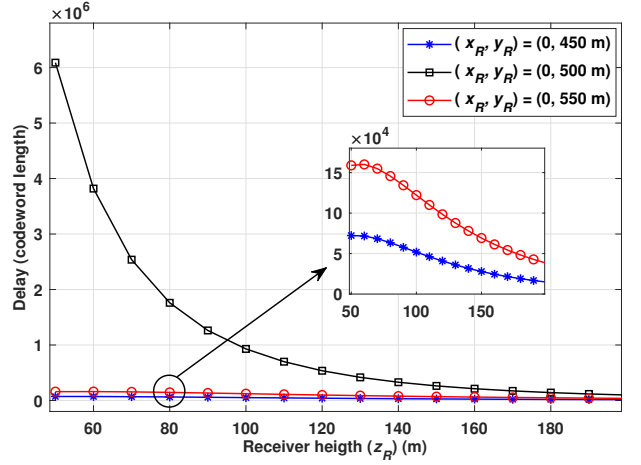
(b) Interference channel with end-to-end received signal-to-noise power ratio $\lambda = 0$ dB.

Fig. 4: Delay profile as a function of the receiver height over different channel conditions (Case II).

- Interestingly, and contrary to the above point, if the UAV is located near the midpoint such that $d_{T,N} \leq d_{i,R}$, increasing the height does not reflect significant changes in the delay.

Figure 5 depicts the delay performance relative to the receiver heights over different channel types for Case III. The results reveal important observations on the delay characteristics, that when the receiver is located in a region near the vicinity of the interfering node, the performance is primarily dominated by interference. Interestingly, as can be seen, the delay decreases with the increasing receiver height for all the curves under all channel conditions. Where the delay values are finite but very high. The higher delay is due to the increasing interference that reduces the success probability of transmission. Moreover, it is to be noted that, irrespective of the channel conditions, the performance is primarily dominated by interference and not by the Gaussian noise.

Given the location of the receiver and the interferer, the minimum delay a G2U communication system must encounter for different values of λ is illustrated in Fig. 6. In obtaining



(a) Interference-limited channel.

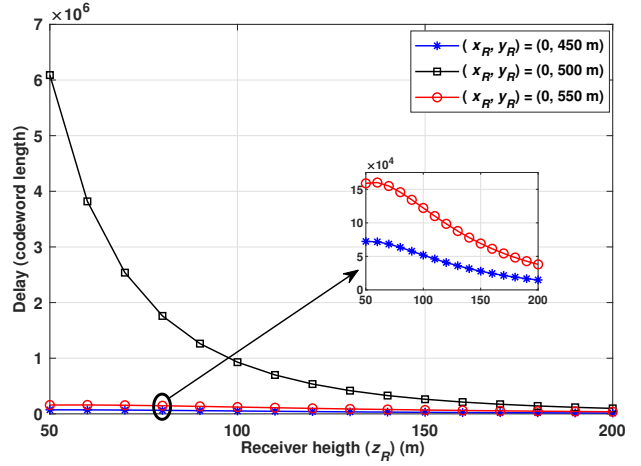
(b) Interference channel with end-to-end received signal-to-noise power ratio $\lambda = 0$ dB.

Fig. 5: Delay profile as a function of the receiver height over different channel conditions (Case III).

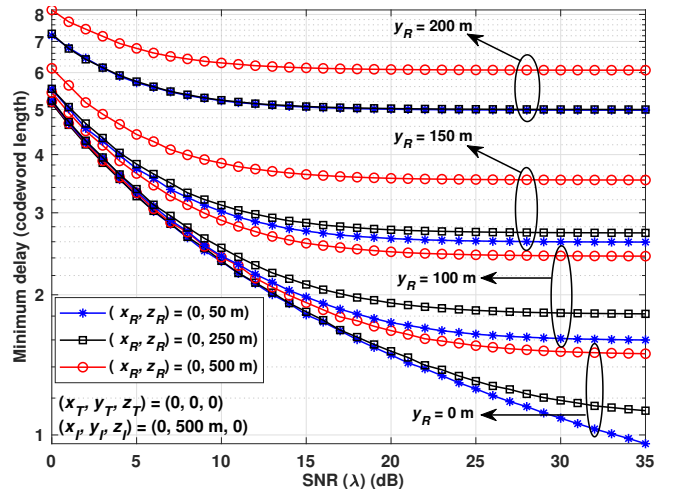


Fig. 6: Minimum delay relative to received SNR for different receiver locations.

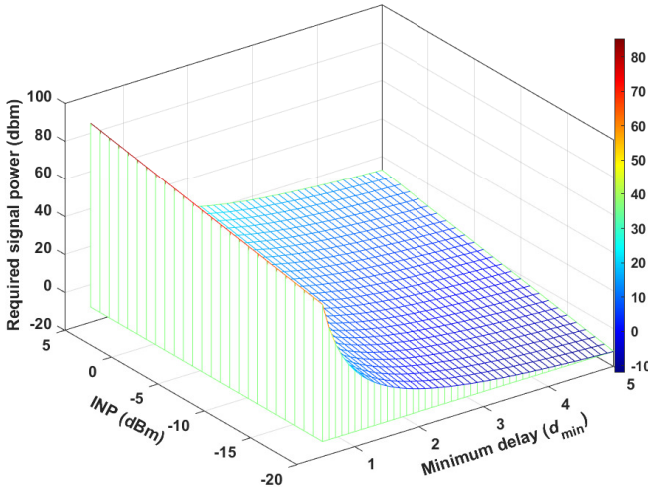


Fig. 7: Delay profile relative to the relay node location.

these curves, the interference power is kept constant at 30 dBm whereas, the reliability constraint is set to 10^{-4} . Following important observations can be made.

- As can be seen, the impact of increasing the signal power in minimizing the transmission delay dominates only if the UAV is located near a region above the transmitter. However, it is to be noted that the negative rate of change of delay with respect to the change in $\bar{\lambda}$ approaches zero for larger values of $\bar{\lambda}$. Moreover, it is also important to note that, as the UAV approaches a region away from the transmitter and near the interferer, the rate $\frac{dd_{c,\min}}{d\bar{\lambda}} \rightarrow 0$ even for smaller values of $\bar{\lambda}$. It shows that increasing $\bar{\lambda}$ gives a negligible gain in terms of minimizing the transmission delay, though may greatly enhance the outage performance.
- As low $\bar{\lambda}$ values, increasing the height of the UAV does not necessarily impact the delay performance. However, as $\bar{\lambda}$ increases, the delay performance degrades with increasing the height.

Given the range of allowable system latency that guarantees that the reliability constraint is met, the minimum transmission power required at the BS for different noise-to-interference power (NIP) levels is illustrated in Fig. 7. In obtaining these results, we fix the location of the receiver and the interferer at $(0, 250, 250)$ and $(0, 500, 0)$, respectively. The reliability constraint is set to $P_e \leq \phi_e = 10^{-4}$. The key observations from the results obtained are as follows:

- Given the reliability constraint and fixed NIP value, there exists a non-linear relation between the allowable transmission delay and the corresponding transmit power requirements. As can be seen, the required transmit power reduces significantly when the allowable transmission delay is relaxed from its initial value. However, on further relaxing the delay requirement, the required transmit power reduces gradually. This phenomenon validates our claim that increasing the signal power beyond a certain limit may not be an optimal solution to the delay minimization problem.
- Given the delay requirement and the reliability constraint,

the required signal power increases with increasing NIP. Importantly, it is to be noted that, this behavior follows a constant rate of change of required transmit power with respect to the change in NIP, irrespective of the delay requirement.

Figure 8 shows the delay profile against the receiver height for different relay node locations. The x_R and y_R coordinates of the receiver are fixed to $(0, 250)$ and are located midway of the line joining the transmitter and the interferer. The amplification gain of the relay UAV is set to -3 dB. However, it is assumed that there is no noise at the input of the relay. For the relay-assisted network, it can be seen that the delay increases with the height initially and then decreases. This phenomenon is more dominating when the relay node is located on the opposite side of the line joining the transmitter and the receiver. Moreover, it can be seen that, as the relay node moves closer to the region between the transmitter and the receiver, the delay performance improves. However, it is to be noted that, as the relay node moves closer to the receiver, the delay though may be lower, but increases with increasing the receiver height. Moreover, for the direct link, as the receiver height increases, there is no impact on the delay performance. Intuitively, this behavior can be attributed to the fact that, if the UAV is located near the region in the middle of the BS and the interferer, changing the UAV height vary the signals strengths from the transmitter and the interferer identically. In obtaining the results in Figs. 8a, 8b, 8c, a few points are important to note.

- For the relayed-assisted network, we assume that there is no direct path between the BS and the receiver UAV. Thus, the relayed UAV in our case serves primarily as compensation for channel degradation due to the path loss and fading between the ground BS and the receiver UAV. Therefore, no additional diversity is achieved in this case.
- The relayed UAV utilizes an amplify-and-forward relaying protocol. Therefore, these results will serve as a lower bound when compared with the conventional decode-and-forward protocol.

The results presented in Fig. 9 are obtained with identical conditions as set in obtaining the results in Fig. 8, however, the relay node is assumed to have Gaussian noise at its input with noise amplification considered.

In Fig. 10, the joint optimization of the relay node and location and the receiver height is presented with the aim to minimize the delay. In obtaining the results in Fig. 10, the end-to-end received average signal-to-noise power ratio is set to -2 dB whereas the amplification gain of the relay node is set to -3 dB. The relay node location index $\{1, 2, 3, 4, 5\}$ corresponds to the location coordinates as $(0, -50, 50)$, $(0, 00, 50)$, $(0, 50, 50)$, $(0, 100, 50)$, $(0, 150, 50)$, respectively. x_R and y_R are set to 0 and 250.

Figure 11 shows the impact of the relay node location in minimizing the delay. Interestingly, it is to be noted that due to the hammock shape of the delay profile, as illustrated in Fig. 11, there is only one global minimum, and the optimal relay node location corresponding to this global minima can readily

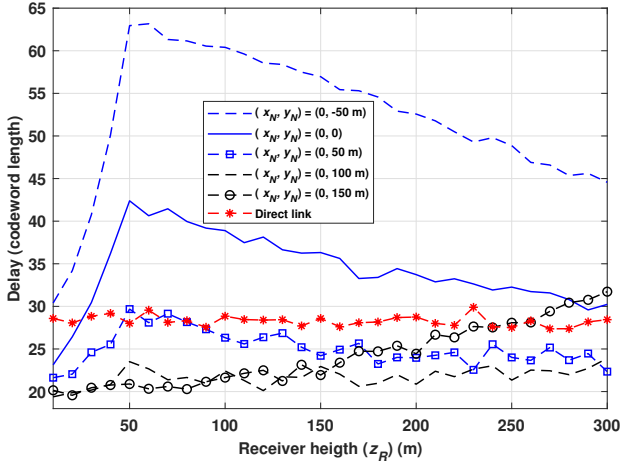
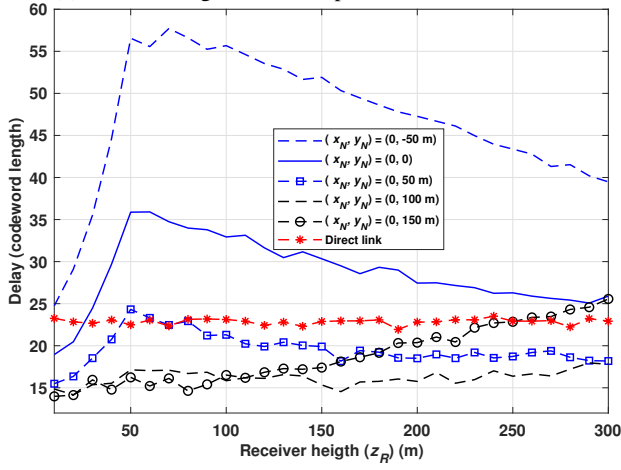
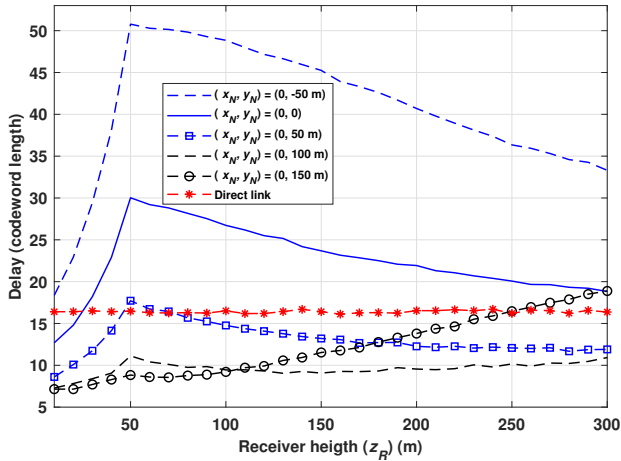
(a) Received signal-to-noise power ratio $\lambda = -2$ dB.(b) Received signal-to-noise power ratio $\lambda = 0$ dB.(c) Received signal-to-noise power ratio $\lambda = 5$ dB.

Fig. 8: Delay profile relative to the relay node location for different receiver heights (without noise amplification at the relay node).

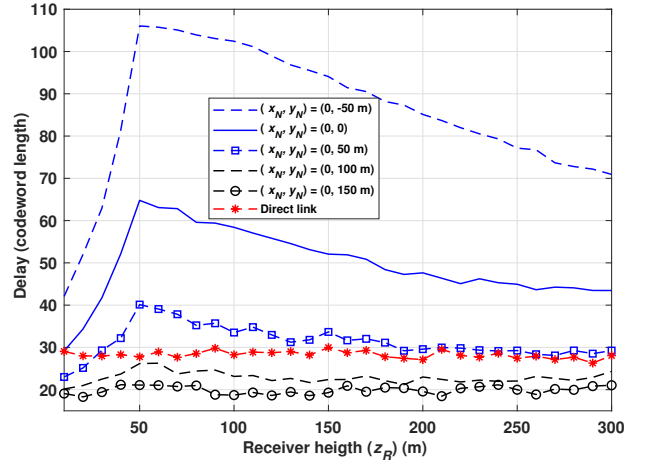
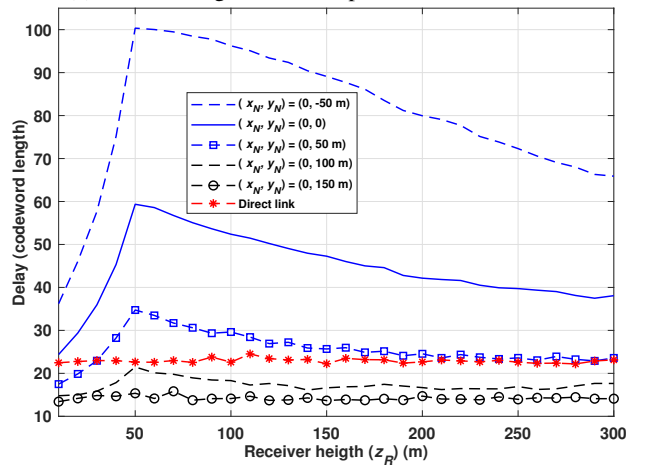
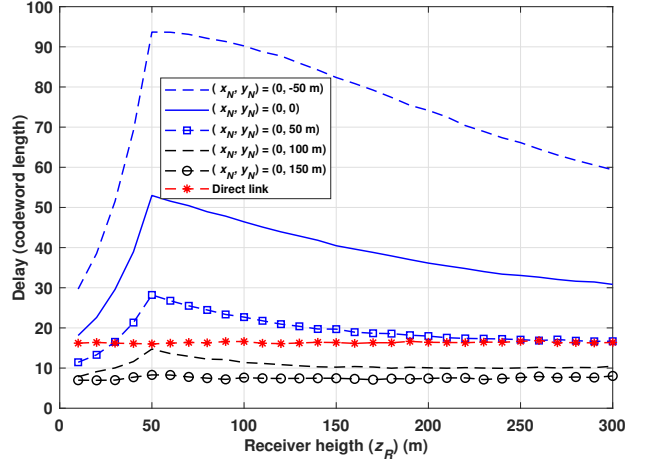
(a) Received signal-to-noise power ratio $\lambda = 5$ dB.(b) Received signal-to-noise power ratio $\lambda = 5$ dB.(c) Received signal-to-noise power ratio $\lambda = 5$ dB.

Fig. 9: Delay profile relative to the relay node location for different receiver heights (with noise amplification at the relay node).

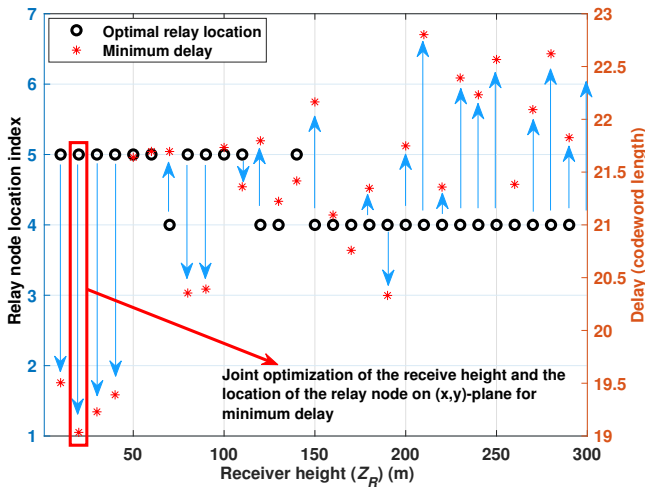


Fig. 10: Optimal link configuration for minimum delay.

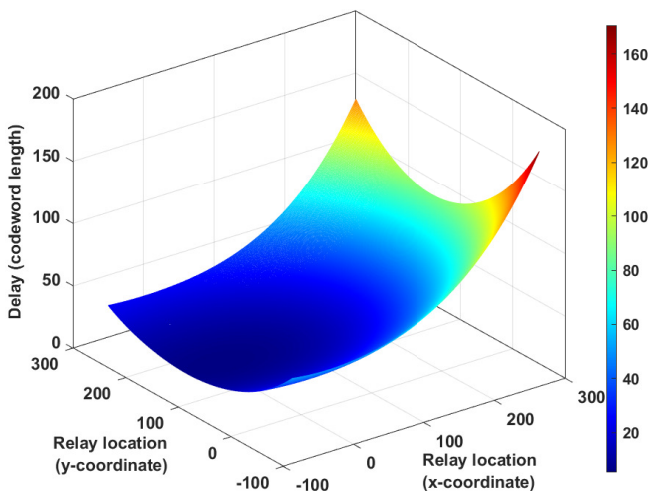


Fig. 11: Delay profile relative to the relay node location.

be obtained using convex optimization. Recall that in obtaining the results in Fig. 11, our dual-hop AF scheme does not exploit the existence of the direct link from the BS to the UAV for the coherent combining of signals at the receiver. Ignoring the direct link in this analysis provides an upper bound on the delay that can be achieved over an interference plus noise G2U channel.

V. CONCLUSION

In this work, we have presented an information-theoretic framework to study the delayed performance of the G2U integrated network. Utilizing Fano's inequality, we have derived the tight upper bound for the channel capacity of the G2U network. Based on the location information of the UAV for a point-to-point G2U, we have also obtained the tight lower bound on the transmit power requirement subject to the reliability constraint and the maximum delay threshold. Interestingly, it has been shown that, despite the simplicity of the point-to-point direct link, the latency of the AF relayed-based link can be lower, if the relay is properly placed. Our results show that increasing the transmit power may not always

be an optimal solution for latency minimization problems, though it may significantly improve the outage performance. A possible extension of this work relates to investigating the ground-to-multi-relayed UAV networks, which can offer higher reliability at the cost of even more system complexity.

APPENDIX PROOF OF (7)

Utilizing (4) and (5) and applying the identities [23, eq. 03.02.26.0006.01] and [23, eq. 01.03.26.0007.01], the average received SNR for the link $u \rightarrow v$ can be expressed as depicted in (18).

Applying the identity [23, eq. 07.34.21.0009.01], and by utilizing the fact that the gamma function has simple poles at negative integers, it can be readily shown that the integral in the Term I in (18) is guaranteed to approach zero irrespective of the values of $\sigma_{h_{u,v}}^2$ and $\rho_{h_{u,v}}^2$. We like to point out that the gamma function is a meromorphic function that has simple poles at negative integers [24]. Finally, applying the identity [23, eq. 07.34.21.0011.01], the integral depicted in Term II can be computed to a closed form as $2 \left(-\sigma_{h_{u,v}}^4 \right) G_{3,4}^{2,1} \left[\frac{2\rho_{h_{u,v}}^2}{\sigma_{h_{u,v}}^2} \middle| \begin{matrix} -2, -1, \frac{1}{2} \\ 0, -2, 0, \frac{1}{2} \end{matrix} \right]$. Substituting the equivalent closed-form expressions corresponding to Term I and Term II in (18), the expression for the average received SNR is obtained as shown in (7).

APPENDIX PROOF OF (16)

Applying the chain rule and utilizing the fact that conditioning reduces entropy, $H(Y_R | S_I)$ can readily be expressed as

$$\begin{aligned}
 H(Y_R | S_I) &\leq \sum_{j=1}^{N_p/T_c} \left\{ \max_{\text{trace}[\mathbb{E}[s_{T,j}, s_{T,j}^*]] \leq T} \mathbb{E} \left[\log(\pi e)^T \right. \right. \\
 &\quad \times \det \left[P_T d_{T,R}^{-\alpha_{T,R}}(\theta_{T,R}) h_{T,R} \mathbb{E} [s_{T,j}, s_{T,j}^*] \right] \\
 &\quad \left. \left. + \sum_{i \in \Phi_I} P_I^{(i)} d_{i,R}^{-\alpha_{i,R}}(\theta_{i,R}) \left[s_{I,j}^{(i)} \left(s_{I,j}^{(i)} \right)^* \right] + B_{TR} N_0 I \right] \right\} \quad (19)
 \end{aligned}$$

where I is the identity matrix. Subscript j represents the block index. It follows that N_p/T_c should be a positive integer. Following a similar approach as illustrated in [25], with some simple mathematical manipulations, (19) can be written as illustrated in (20).

Utilizing the chain rule for entropy, $H(Y | S, s_I)$ can readily be expressed as shown in (21). Applying the Markov chain, the expression in (21) is reduced to the expression as illustrated in (22).

$$\begin{aligned}
 H(Y | S, s_I) &= \\
 &N_p \log(\pi e) + \frac{N_p (T_c - 1)}{T_c} \log(B_{TR} N_0) \\
 &+ \sum_{j=1}^{N_p/T_c} \mathbb{E}_{s_{I,j}} \log \left(\sum_{i \in \Phi_I} P_I^{(i)} d_{i,R}^{-\alpha_{i,R}}(\theta_{i,R}) \left\| s_{I,j}^{(i)} \right\|^2 + w_R \right) \quad (22)
 \end{aligned}$$

$$\begin{aligned}
H(Y_R | s_I) &\leq N_p \log(\pi e) + \frac{N_p(T_c - 1)}{T_c} \log\left(P_T d_{T,R}^{-\alpha_{T,R}(\theta_{T,R})} + B_{TR} N_0\right) \\
&+ \sum_{j=1}^{N_p/T_c} E_{s_{I,j}} \left[\log\left(P_T d_{T,R}^{-\alpha_{T,R}(\theta_{T,R})} + \sum_{i \in \Phi_I} P_I^{(i)} d_{i,R}^{-\alpha_{I,R}(\theta_{I,R}^{(i)})} \|s_{I,j}^{(i)}\|^2 + B_{TR} N_0\right) \right].
\end{aligned} \tag{20}$$

$$\begin{aligned}
H(Y_R | S, s_I) &= \sum_{j=1}^{N_p/T_c} H(y_j | y_1, \dots, y_{j-1}, S, s_I) \\
&= \sum_{j=1}^{N_p/T_c} H\left(\sum_{i \in \Phi_I} \sqrt{P_I^{(i)} d_{i,R}^{-\alpha_{I,R}(\theta_{I,R}^{(i)})}} h_{I,j}^{(i)} s_{I,j}^{(i)} + w_R \middle| y_1, \dots, y_{j-1}, S, s_I\right).
\end{aligned} \tag{21}$$

Substituting (20) and (22) into (10), and applying simple mathematical manipulations, yields (16).

REFERENCES

- [1] Ma Zheng, Xiao Ming, Xiao Yue, Pang Zhibo, Poor H Vincent, and Vucetic Branka, "High-reliability and low-latency wireless communication for internet of things: Challenges, fundamentals, and enabling technologies," *IEEE Internet of Things Journal*, **6** (5), (2019) 7946–7970.
- [2] Popovski Petar, Stefanović Cedomir, Nielsen Jimmy J, De Carvalho Elisabeth, Angelichinoski Marko, Trillingsgaard Kasper F, and Bana Alexandru-Sabin, "Wireless access in ultra-reliable low-latency communication (URLLC)," *IEEE Transactions on Communications*, **67** (8), (2019) 5783–5801.
- [3] Shirvanimoghaddam Mahyar, Mohammadi Mohammad Sadegh, Abbas Rana, Minja Aleksandar, Yue Chentao, Matuz Balazs, Han Guojun, Lin Zihuai, Liu Wanchun, and Li Yonghui, "Short block-length codes for ultra-reliable low latency communications," *IEEE Communications Magazine*, **57** (2), (2018) 130–137.
- [4] Muruganathan Siva D, Lin Xingqin, Määtänen Helka-Liina, Sedin Jonas, Zou Zhenhua, Hapsari Wuri A, and Yasukawa Shinpei, "An overview of 3GPP release-15 study on enhanced LTE support for connected drones," *IEEE Communications Standards Magazine*, **5** (4), (2021) 140–146.
- [5] Zeng Yong, Lyu Jiangbin, and Zhang Rui, "Cellular-connected UAV: Potential, challenges, and promising technologies," *IEEE Wireless Communications*, **26** (1), (2018) 120–127.
- [6] Lin Xingqin, Yajnanarayana Vijaya, Muruganathan Siva D, Gao Shiwei, Asplund Henrik, Maattanen Helka-Liina, Bergstrom Mattias, Euler Sebastian, and Wang Y-P Eric, "The sky is not the limit: LTE for unmanned aerial vehicles," *IEEE Communications Magazine*, **56** (4), (2018) 204–210.
- [7] Tran Dinh-Hieu, Nguyen Van-Dinh, Chatzinotas Symeon, Vu Thang X, and Ottersten Björn, "UAV relay-assisted emergency communications in IoT networks: Resource allocation and trajectory optimization," *IEEE Transactions on Wireless Communications*, **21** (3), (2021) 1621–1637.
- [8] Hosseinalipour Seyyedali, Rahmati Ali, and Dai Huaiyu, "Interference avoidance position planning in dual-hop and multi-hop UAV relay networks," *IEEE Transactions on Wireless Communications*, **19** (11), (2020) 7033–7048.
- [9] Salehi Fateme, Ozger Mustafa, Neda Naaser, and Cavdar Cicek, "Ultra-Reliable Low-Latency Communication for Aerial Vehicles via Multi-Connectivity," *IEEE 2022 Joint European Conference on Networks and Communications & 6G Summit (EuCNC/6G Summit)*, (2022) 166–171.
- [10] Ladosz Pawel, Oh Hyondong, and Chen Wen-Hua, "Optimal positioning of communication relay unmanned aerial vehicles in urban environments," *IEEE 2016 International Conference on Unmanned Aircraft Systems (ICUAS)*, (2016) 1140–1147.
- [11] Faqir Omar J, Nie Yuanbo, Kerrigan Eric C, and Gündüz Deniz, "Energy-efficient communication in mobile aerial relay-assisted networks using predictive control," *Elsevier IFAC-PapersOnLine*, **51** (20), (2018) 197–202.
- [12] Zeng Yong, Zhang Rui, and Lim Teng Joon, "Throughput maximization for UAV-enabled mobile relaying systems," *IEEE Transactions on communications*, **64** (12), (2016) 4983–4996.
- [13] Ono Fumie, Ochiai Hideki, and Miura Ryu, "A wireless relay network based on unmanned aircraft system with rate optimization," *IEEE Transactions on Wireless Communications*, **15** (11), (2016) 7699–7708.
- [14] Rahmati Ali, Yapici Yavuz, Rupasinghe Nadisanka, Guvenc Ismail, Dai Huaiyu, and Bhuyan Arupjyoti, "Energy efficiency of RSMA and NOMA in cellular-connected mmWave UAV networks," *IEEE 2019 IEEE International Conference on Communications Workshops (ICC Workshops)*, (2019) 1–6.
- [15] Wang Ying, Gorski Adam, and da Silva Aloizio Pereira, "Development of a data-driven mobile 5g testbed: Platform for experimental research," *2021 IEEE International Conference on Communications and Networking (MeditCom)*, (2021) 324–329.
- [16] Series P, "Propagation data and prediction methods required for the design of terrestrial broadband radio access systems operating in a frequency range from 3 to 60 GHz," *Recommendation ITU-R*, (2013) 1410–1415.
- [17] Gradshteyn Izrail Solomonovich, and Ryzhik Iosif Moiseevich, "Table of integrals, series, and products," *Academic press*, (2014).
- [18] Gallager Robert G, "Information theory and reliable communication," *Springer*, **588** (1968).
- [19] Adamchik Victor S, and Marichev OI, "The algorithm for calculating integrals of hypergeometric type functions and its realization in REDUCE system," *Proceedings of the international symposium on Symbolic and algebraic computation*, **588** (1990) 212–224.
- [20] Tse David, and Viswanath Pramod, "Fundamentals of wireless communication," *Cambridge university press*, (2005).
- [21] Scarlett Jonathan, and Cevher Volkan, "An introductory guide to Fano's inequality with applications in statistical estimation," *arXiv preprint arXiv:1901.00555*, (2019).
- [22] Kim Minsu, and Lee Jemin, "Outage probability of UAV communications in the presence of interference," *2018 IEEE Global Communications Conference (GLOBECOM)*, (2018) 1–6.
- [23] "The Wolfram Functions Site Wolfram Research, Inc.," <http://functions.wolfram.com>.
- [24] Thukral Ashwani K, "Factorials of real negative and imaginary numbers-A new perspective," *SpringerPlus*, **3** (1), (2014) 1–13.
- [25] Zhang Shengli, Liew Soung Chang, and Chen Jinyuan, "The capacity of known interference channel," *IEEE Journal on Selected Areas in Communications*, **33** (6), (2015) 1241–1252.



Sudhanshu Arya (Member, IEEE) is a researcher in the School of System and Enterprises at Stevens Institute of Technology, NJ, USA. He received his M.Tech. degree in communications and networks from the National Institute of Technology, Rourkela, India, in 2017, and the Ph.D. degree from Pukyong National University, Busan, South Korea, in 2022. He worked as a Research Associate with the Department of Artificial Intelligence Convergence, at Pukyong National University. His research interests include wireless communications and digital signal processing, with a focus on free-space optical communications, optical scattering communications, optical spectrum sensing, computational game theory, and artificial intelligence. He received the Best Paper Award in ICGHIT 2018 and the Early Career Researcher Award from the Pukyong National University in 2020.



Ying Wang (Member, IEEE) received the B.E. degree in information engineering at Beijing University of Posts and Telecommunications, M.S. degree in electrical engineering from University of Cincinnati and the Ph.D. degree in electrical engineering from Virginia Polytechnic Institute and State University. She is an associate professor in the School of System and Enterprises at Stevens Institute of Technology. Her research areas include cybersecurity, wireless AI, edge computing, health informatics, and software engineering.